X-RAY BURSTS FROM THE GALACTIC X-RAY TRANSIENT SOURCE GRS 1915+105

J. S. Yadav[1], and A. R. Rao[1]

[1] *Tata Institute of Fundamental Research, Homi Bhabha Road, Mumbai, 400 005, India*

ABSTRACT

We have analyzed publicly available RXTE/PCAs archival data of GRS 1915+105 during its burst/flaring state. The burst cycle ranges from 30 to 1300 s. These bursts are different from the type I and type II classical bursts seen in Low Mass X-ray Binaries (LMXBs) in terms of their temporal and spectral properties. We have classified these bursts on the basis of properties observed during the quiescent (low flux) phase. The 2 - 10 Hz QPOs are present during the quiescent phase and disappear during the burst phase of all types of these X-ray bursts. The duration of the quiescent phase can be explained assuming an outflow from the post-shock regions and the catastrophic Compton cooling.

INTRODUCTION

The Galactic X-ray transient source GRS 1915+105 has shown spectacular X-ray variability during last four years of its observation by RXTE and other satellites (Greiner et al. 1996, Yadav et al. 1999, Belloni et al. 2000). This source was discovered in 1992 with the WATCH all sky X-ray monitor onboard the GRANAT satellite (Castro-Tirado et al. 1994). The X-ray intensity was found to vary on a variety of time scales and the light curve showed a complicated pattern of dips and rapid transitions between high and low intensity (Belloni et al. 1997, Taam et al. 1997). Recently, Yadav et al. (1999) have made a detailed study of various types of X-ray bursts seen in GRS 1915+105 from IXAE/PPCs observations during 1997 June - August and have suggested that during the bursts the source switches back and forth between the low-hard state and the high-soft state near critical accretion rates in a very short time scale. The fast time scale for the transition of the state is explained by invoking the appearance and disappearance of the advective disk in its viscous time scale.

In this paper, we present results of our analysis of a set of publicly available RXTE/PCA observations of GRS 1915+105 during last four years which samples a broad range of burst cycles from 30 s to 1300 s. Each burst cycle consists of a low flux quiescent phase followed by a high flux burst phase and the fast transition

Table I.
Summary of selected observations of GRS 1915+105

Observation ID	Date (UT)	Exposure (s)	Type of Bursts	ASM[a] Flux	Rec. Time (s)	Av. Q. Flux	Remark
10408-01-01-01	1996 April 06 05:40	5600	Regular (R2)	99.4	280[b]	6200	QT $\sim$ 20 s
10408-01-38-00	1996 Oct 07 05:44	7000	Regular (R3)	98.8	1150[b]	3200	-
20402-01-30-00	1997 May 26 12:25	3215	Regular (R1b)	47.6	105[b]	7500	BT $\sim$ 20 s
20402-01-33-00	1997 June 18 14:17	3472	Irregular (IR)	61.5	var.	var.	-
20402-01-34-01	1997 June 22 19:27	2550	Regular (R1a)	59.7	55[b]	8700	BT $\sim$ 20 s

QT = quiescent time, BT = burst time, Av. Q. Flux= average quiescent time flux (c/s), var. = variable
[a] Mean ASM flux (c/s) for a day, [b] Mean burst recurrence time

in less than 10 s. We include here only those bursts which have dips or quiescent phase with hard spectrum (Yadav 2001, Yadav & Rao 2001).

OBSERVATIONS

We have selected a set of observations from publicly available RXTE/PCA data for the X-ray transient source GRS 1915+105 (Jahoda et al. 1996). The source was in high/flaring state during these observations. The dips or the quiescent phase in these observations are spectrally hard while the brighter portions (the burst phase) are soft. A portion of 2−13 keV light curves for different days added for all PCA units (except on 1996 April 6, when only three PCA units were on), are shown in Figure 1. In Table 1 we list details of these observations alongwith some of the properties of the observed X-ray bursts. During these observations ASM flux varies from 47 to 100 ASM c/s while the quiescent time flux varies in the range of 3000−10000 c/s (added for 5 PCA units) in the 2−13 keV energy range.

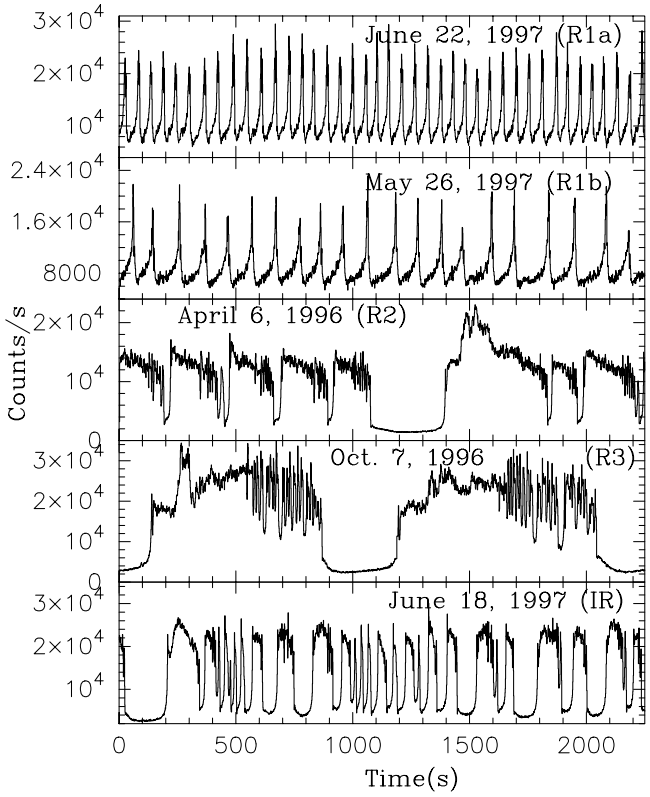

Fig. 1. The regular bursts with ∼ 55 s recurrence time (first panel from the top), regular bursts with ∼ 105 s recurrence time (second panel), regular bursts with ∼ 280 s (third panel), regular bursts with ∼ 1150 s recurrence time (fourth panel), and irregular bursts (fifth panel) observed in GRS 1915+105 with all the PCAs except on 1996 April 6 when only three PCA units were on.

RESULTS AND DISCUSSION

These bursts can broadly be put into two classes: regular bursts centered around a fixed period with low dispersion ($\delta P/P \sim 1-50\%$) and irregular bursts with no fixed periodicity ($\delta P/P > 50\%$). The observed bursts are classified into four types: (1) regular bursts (R1) with short burst phase lasting for ∼ 20 s and recurring every 50−145 s (extreme ends of this type are shown in first and second panels from top of Figure 1 (R1a type and R1b type respectively), for other bursts of this type see Vilhu & Nevalainen (1998)). These bursts have lowest dispersion ($\delta P/P \sim 1-10\%$), (2) regular bursts (R2) with short quiescent phase lasting for ∼ 20 s recurring every 280 s (third panel from top). The $\delta P/P$ is upto 50% for these bursts, (3) long regular bursts (R3) recurring every 1150 s (fourth panel from top). The $\delta P/P$ is upto 15% for these bursts, and (4) irregular bursts (IR) with duration of a few tens to a few hundred seconds (bottom panel of Figure 1). The regular bursts with short burst phase usually have two-peak structure while irregular and long regular bursts show multi-peak structure with higher variability near the end of the burst.

The most striking features of these bursts are slow exponential rise, sharp linear decay and hardening of spectrum as burst progresses (Paul et al. 1998). The decay time scales are shorter than the rise time scales. In sharp contrast, the decay time is longer than the rise time in classical bursts and spectrum is initially hard and becomes softer as the burst decays. The ratio of luminosity in type I X-ray bursts (L_b) and the average quiescent X-ray luminosity (L_q) is $\frac{L_b}{L_q} \sim 10^{-2}$. The time-averaged type II burst luminosity is higher, usually 0.4 to 2.2 times the average luminosity of quiescent emission (Lewin et al. 1995). The time-averaged luminosity of the bursts seen in GRS 1915+105 is found to be from 0.15 to 4.5 times the average luminosity of the quiescent emission. The emission process involved in producing these bursts is likely to be gravitational as in the case of type II bursts due to the energetics involved, but the large value of this ratio indicates the black hole nature of the compact object where more gravitational potential energy is available.

Yadav et al. (1999) have suggested that the source is in a high-soft state during the burst phase and in a low-hard state during the quiescent phase on the basis of available spectral observations and derived disk parameters of GRS 1915+105. The source makes state transitions in very short time scales corresponding to the rise and fall time of the bursts (a few seconds). Such fast changes of states are possible in the Two Component Accretion Flows (TCAF) where the advective disk covers the standard thin disk (Chakrabarti 1996, Rao et al. 2000). The time scales of the burst phase are compared with the viscous time scales of the thin accretion disk. Recently, Chakrabarti (1999) have presented a solution to the rapid state transition based on TCAF (Chakrabarti & Titarchuk 1995). The mass outflow from the regions of the shock compressed flow initiates the quiescent phase and the catastrophic Compton cooling of the material in the sonic sphere marks the end of the quiescent phase and the start of the burst phase. This model essentially reinforces the suggestion of Yadav et al. (1999) but gives a physical basis for the start of the event. The shock compressed gas with compression ratio R > 1 will produce the outflows which pass through the sonic points at $R_c = f_o \times R_s$ provided the flow is isothermal till R_c, where R_s is the shock location and $f_o = R^2/(R-1)$ (Chakrabarti 1999). Chakrabarti & Manickam (2000) have expanded this model further and derived a correlation between t_{off} the duration of off state (duration in which the sonic sphere becomes ready for catastrophic Compton cooling) and ν_I the QPO frequency between 2 − 10 Hz. For an average shock $2.5 < R > 3.3$, t_{off} is insensitive to the compression ratio. Using average value of R = 2.9 and a constant velocity post-shock flow $\alpha = 1$ following relation is derived between t_{off} and ν_I;

$$t_{off} = 461.5 \left(\frac{0.1}{\Theta_{\dot{M}}}\right) \left(\frac{m}{10}\right)^{-1} \left(\frac{v_o}{0.066}\right)^2 \nu_I^{-2} s. \quad (1)$$

where m is the mass of the black hole in units of the solar mass m = 10, $v_o = 0.066$, and $\Theta_{\dot{M}}$ is a dimensionless parameter defined as $\Theta_{\dot{M}} = (\Theta_{out}/\Theta_{in}) \times \dot{m}_d$ where Θ_{in} and Θ_{out} are the solid angles of the inflow & outflow respectively and $\dot{m}_d$ is the disk accretion rate in units of Eddington accretion rate. In this configuration $\dot{m}_h \sim 1$ and $\dot{m}_d \sim 0.1$ keeping the total accretion rate $\dot{m}_t$ close to 1.

In Figure 2, we plot Eq. 1 in the log - log scale taking t_{off} as the quiescent time for $\Theta_{\dot{M}} =$ 0.0145, 0.0245 and 0.0335. We searched for QPO peaks in the PDS by fitting frequency intervals between 0.5−10 Hz with Gaussian profiles on top of a power-law background continuum. The width and position of the Gaussian are kept as free parameters. Results are plotted in Figure 2. The data of bursts with quiescent time in a narrow range are clubbed together to improve the statistics of PDS analysis. The errors in QPO frequency is less than the size of the symbols. Although we have used almost similar number of bursts for R1 (a & b), IR and R3 bursts as used by Chakrabarti & Manickam (2000), the data points are reduced in our case. We have added the R2 bursts to this analysis which have enabled us to investigate the inverse-square law dependence over a range of 25−320 s (dotted line). In comparison, Chakrabarti & Manickam (2000) have few points around 320 s. These results are in good agreement. The data points

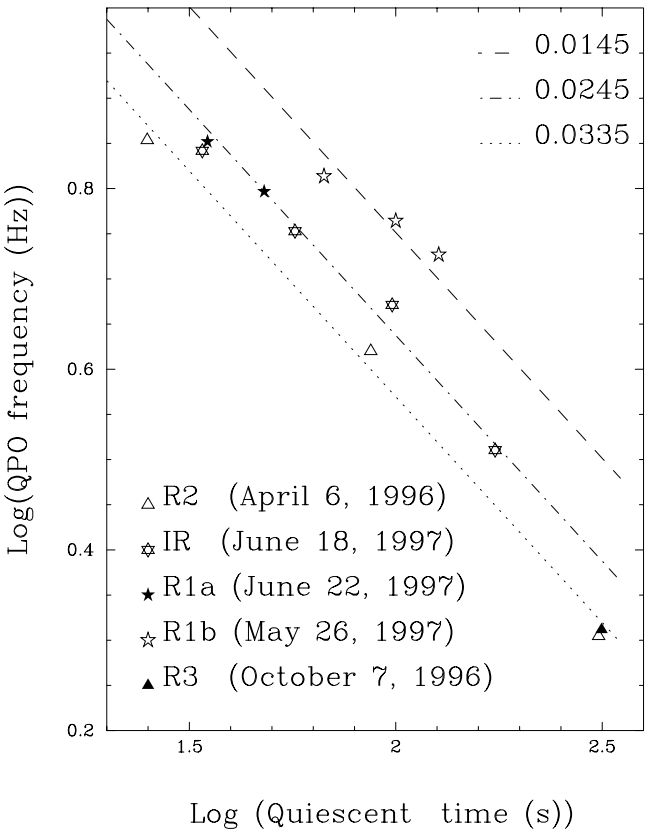

Fig. 2. Variation of QPO frequency ν_I (minimum) with the quiescent time for different types of X-ray bursts observed in GRS 1915+105 (data points). Plotted lines are the quiescent time $\alpha\ \nu_I^{-2}$ for different values of $\Theta_{\dot{M}}$ (for further details see in text).

of R2 and R3 bursts when ASM flux was 99.4 & 98.8 c/s respectively fall along the dotted line with $\Theta_{\dot{M}} =$

0.0335. The data points of R1a and IR bursts when ASM flux was 59.7 and 61.5 c/s respectively fall along the dashed - dotted line ($\Theta_{\dot{M}} = 0.0245$). The data points of R1b bursts during which ASM flux has lowest value of 47.6 c/s fall along the dashed line ($\Theta_{\dot{M}} = 0.0145$). It may be noted here that the $\Theta_{\dot{M}}$ and the ASM flux though determined independently agree well for different types of bursts as both of these are related to the disk accretion rate $\dot{m}_d$.

Our results in Figure 2 suggest that the t_{off} represents the quiescent time of all the bursts which may or may not be of the order of the viscous time scales of the thin accretion disk. However non-zero burst time would represent the viscous time scales of the thin accretion disk as any change in the $\dot{m}_d$ would require the viscous time scale to reach R_c when system can revert back to the quiescent phase (Yadav et al. 1999). The IR bursts are produced due to viscous - thermal - instability and the quiescent and burst time are correlated suggesting that both these parameters represent the viscous time scales of the thin disk (t_{off} is of the order of viscous time scales and changing continuously). The burst time varies over a large range of 100 to 500 s suggesting viscous - thermal condition are not stable during R2 bursts. The dispersion around a fixed period is large ($\delta P/P$ is upto 50 %). The burst duration of R3 bursts fall in a range of 700 to 1000 s suggesting fairly stable viscous - thermal conditions during R3 bursts. The quiescent time is fixed during R2 and R3 bursts ($\sim$ 20 & $\sim$ 320 s respectively) which represents t_{off}.

The R1 bursts seen on 1997 May 26 and 1997 June 22 termed as "ringing flares" have a short burst phase of $\sim$ 20 s. The peak flux during the burst phase lasts only for 1 - 2 s . The quiescent time properties of these bursts are very different from the properties observed for other types of bursts. The average quiescent flux is high (7000−10000 c/s) and the Γ of the energy spectrum is 2.67. The ASM flux is low (47−60 ASM c/s). The HR_1 (ratio of flux in 5−13 keV band and flux in 2−5 keV band) is high (1.0−1.06) during the quiescent phase. The ratio of the average burst flux and the average quiescent flux is almost constant during these bursts (Yadav & Rao 2001). The dispersion around a fixed period is lowest ($\delta P/P \sim 1 - 10\%$). This type of bursts have been observed for extended period almost continuously from 1997 May 26 to June 26 suggesting very stable thermal - viscous conditions during these burst (Yadav et al. 1999, Yadav & Rao 2001). At t_{off}, the sonic sphere cools down which ends the quiescent phase and marks the start of the burst phase. However the conditions are very stable and remain unchanged. The outflows immediately start and sub-Keplerian halo appears quickly which abruptly ends the burst phase and the next quiescent phase starts producing ringing type burst phase with the burst peak flux hardly lasting for 1 - 2 s. The quiescent time decreases as the $\dot{m}_d$ increases (Figure 2). As the average quiescent flux increases the t_{off} decreases reducing the burst recurrence time without affecting the burst phase duration. An increase in the $\dot{m}_d$ increases the quiescent flux and reduces the burst cycle (appearing of the burst phase more frequently) which explains why this type of bursts were observed over a large range of ASM flux from 47 to 60 c/s (the HR_1 remains unchanged).

REFERENCES

Belloni, T., M. Mendez, A. R. King, M. van der Klis, and J. Paradijs, A Unified Model for the Spectral Variability in GRS 1915+105, *ApJ*, **488**, L109-113, 1997.

Belloni, T., M. Klein-Wolt, M. Mendez, M. van der Klis, and J. Paradijs, A model-independent analysis of the variability of GRS 1915+105, *A & A*, **355**, 271-290, 2000.

Castro-Tirado, A. J., S. Brandt, N. Lund, I. Lapshov, R. A. Sunyaev, A. A. Shyapnikov, A. Aleksei, S. Guziy, and E. P. Pavlenko, Discovery and observations by watch of the X-ray transient GRS 1915+105, *ApJS*, **92**, 469-472, 1994.

Chakrabarti, S. K., Accretion processes on a black hole, *Phys. Rep.*, **266**, 229-390, 1996.

Chakrabarti, S. K., Estimation and effects of the mass outflow from shock compressed flow around compact objects, *A & A*, **351**, 185-191, 1999.

Chakrabarti, S. K., and S. G. Manickam , Correlation among Quasi-Periodic oscillation Frequencies and Quiescent state duration in Black Hole Candidate GRS 1915+105, *ApJl*, **531**, L41-45, 2000.

Chakrabarti, S. K., and L. G. Titarchuk, Spectral properties of accretion disks around Galactic and Extragalactic Black Holes, *ApJ*, **455**, 623-639, 1995.

Greiner, J., E. H. Morgan, and R. A. Remillard, Rossi X-Ray Timing Explorer observations of GRS 1915+105, *ApJ*, **473**, L107-110, 1996.

Jahoda, K., J. H. Swank, A. B. Giles, M. J. Stark, Tod. Strohmayer et al., In-orbit performance and calibration of the Rossi X-ray Timing Explorer (RXTE) Proportional Counter Array (PCA), Proc. SPOE Vol 2808 , EUV, X-ray and Gamma rays instrumentation in Astronomy VII, Eds. O. H. Siegmund & M. A. Gummin, 59-70, 1996.

Lewin, W. H. G., Jan Van Paradijs, & Taam, R. E., in X-ray Binaries, Eds. Lewin., W. H. G., Jan Van Paradijs, & van den Heuvel, Cambridge: Cambridge University Press, p. 175-232, 1995.

Taam, R. E., X. Chen,, & J. H. Swank, Rapid Bursts from GRS 1915+105 with RXTE, *ApJ*, **485**, L83-86, 1997.

Paul, B., P. C. Agrawal, A. R. Rao, M. N. Vahia, J. S. Yadav et al., Quasi-regular X-ray bursts from GRS 1915+105 observed with the IXAE: possible evidence for matter disappearing into the event horizon of the black hole, *ApJ*, **492**, L63-67, 1998.

Rao, A. R., J. S. Yadav, & B. Paul, Rapid Satae transitions in the Galactic black hole candidate source GRS 1915+105, *ApJ*, **544**, 443-452, 2000.

Vilhu, O. & J. Nevalainen, Two-phase modeling of the rings in the RXTE two-color diagram of GRS 1915+105, *ApJ*, **508**, L85-88, 1998.

Yadav, J. S., A. R. Rao, P. C. Agrawal, B. Paul, S. Seetha et al., Different types of X-ray bursts from GRS 1915+105 and their origin, *ApJ*, **517**, 935-950, 1999.

Yadav, J. S., Disk-jet connection in the microquasar GRS 1915+105 and IR and radio emission, *ApJ*, **548**, 876, 2001.

Yadav, J. S. & A. R. Rao, X-ray flares/bursts from GRS 1915+105 and the two component accretion flow, *Astrophysics and Space Science*, in press, 2001.